A Fast, Numerical Circuit-Level Model of Carbon Nanotube Transistor

Tom J Kazmierski, Dafeng Zhou and Bashir M Al-Hashimi
School of Electronics and Computer Science
University of Southampton
Southampton, SO17 1BJ,UK
tjk,dz05r,bmah@ecs.soton.ac.uk

Abstract

Recently proposed circuit-level models of carbon nanotube transistor (CNT) for SPICE-like simulators suffer from numerical complexities as they rely on numerical evaluation of integrals or internal Newton-Raphson iterations to find solutions of non-linear dependencies or both. Recently an approach has been proposed which eliminates the need for numerical integration when calculating the charge densities in CNTFET through the use of piece-wise linear approximation. This paper builds on the effective employment of linear approximation to accelerate the CNT model speed when evaluating the source-drain current of the CNT, but rather than using symbolic solutions as reported, we propose to employ a numerical linearization of charge density dependence on the self-consistent voltage to obtain a dramatic reduction in the CPU time. Our results show a speed up of up to almost four orders of magnitude compared with the theoretical CNT model implemented in FETToy, used as a reference for verifying newer models. Comparisons of drain-source current characteristics of the new model against that in FETToy are presented, confirming the accuracy of the proposed approach.

1. Introduction

While it is gradually becoming more clear how the Carbon Nanotube Transistor (CNT) operates [1, 2], several SPICE-compatible models have recently been proposed (eg. [3, 4, 5, 6, 7, 8]) in anticipation that analog and digital systems built with CNT devices will soon need to be simulated at the circuit level. Most proposed models rely on an estimation of the mobile charge densities from which the total drain current is derived [1]. Accurate calculation of the mobile charge involves integrating the densities of states over the number of allowed energy levels using the Fermi probability distribution. As the total drain-source current is driven by the self-consistent voltage, which comprises i.a. the drain-source bias voltage as well as potential induced by the non-equilibrium mobile charge injected from the source and drain, a solution of non-linear algebraic equations is necessary to calculate the drain current. Numerical evaluations of integrals and iterative solutions of non-linear algebraic equations (usually by the Newton-Raphson approach) are time consuming and may be impractical in simulations involving large numbers of CNT devices of varying parameters. The well known MATLAB script named FETToy [9] requires more than 12 seconds of the CPU time on a Pentium IV based PC to calculate a family of CNT current drain characteristics. A recent interesting approach [8] proposes a piece-wise linear approximation of the charge density profiles to simplify calculations. In this contribution we further simplify and generalize the charge density linearization and obtain a speed-up of approximately 8000 times, which represents almost four orders of magnitude, compared with FETToy. As our results demonstrate, the loss of accuracy due to charge density linearization is insignificant.

2. Fast circuit-level CNT model

When a voltage $V_{DS} > 0$ is applied to the drain and source of a top-gate or a bottom-gate CNT [10, 11] the following non-equilibrium mobile charge density is induced [1]

$$\Delta Q = q(N_S + N_D - N_0) \tag{1}$$

where N_S is the density of positive velocity states filled by the source, N_D is the density of negative velocity states filled by the drain and N_0 is the equilibrium electron density. These densities are given by

$$N_S = \frac{1}{2}\int_{-\infty}^{+\infty} D(E)f(E - U_{SF})dE \tag{2}$$

$$N_D = \frac{1}{2}\int_{-\infty}^{+\infty} D(E)f(E - U_{DF})dE \tag{3}$$

$$N_0 = \int_{-\infty}^{+\infty} D(E) f(E - E_F) dE \quad (4)$$

where U_{SF} and U_{DF} are defined as

$$U_{SF} = E_F - qV_{SC} \quad (5)$$

$$U_{DF} = E_F - qV_{SC} - qV_{DS} \quad (6)$$

V_{SC} is the self-consistent voltage, $D(E)$ is the density of states,E_f is the Fermi level, f is the Fermi probability distribution, q is the electronic charge and E represents the energy levels per CNT unit length.

The self-consistent voltage V_{SC} is derived from the total device charge density and hence must be calculated using an implicit relationship. This relationship is given by the following equation [8]

$$V_{SC} = -\frac{Q_t + qN_S(V_{SC}) + qN_d(V_{SC}) + qN_0}{C_\Sigma} \quad (7)$$

where Q_t represents the charge stored in terminal capacitances and is defined as

$$Q_t = V_G C_G + V_D C_D + V_S C_S \quad (8)$$

where C_G, C_D, C_S are the gate, drain, and source capacitances correspondingly and the total terminal capacitance C_Σ is

$$C_\Sigma = C_G + C_D + C_S \quad (9)$$

For the purpose of circuit modeling, we propose to apportion equal parts of the equilibrium mobile charge density N_0 to the drain and source, and introduce the corresponding non-equilibrium mobile charge densities Q_S and Q_D as follows

$$Q_S(V_{SC}) = q(N_S - \frac{1}{2}N_0) \quad (10)$$

and

$$Q_D(V_{SC}) = q(N_D - \frac{1}{2}N_0) \quad (11)$$

The non-equilibrium mobile charges can now be represented as circuit capacitances as shown in the equivalent circuit of the model in figure 1 connected between the drain and source correspondingly and the inner node Σ that represents a hypothetical point which combines all the CNT charges that affect the self-consistent voltage and hence the drain-source current I_{DS}. As in our model the self-consistent voltage V_{SC} is a piece-wise linear function of the terminal voltages V_G, V_S and V_D, the capacitances which

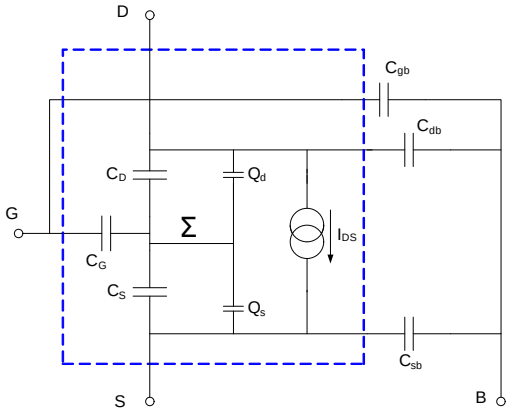

Figure 1. Equivalent circuit for the proposed CNT model.

store the source and drain mobile charges Q_S and Q_D are also piece-wise linear and controlled by the terminal voltages.

As it has already been highlighted in Introduction above, evaluation of the self-consistent voltage directly from equation (7) involves a time consuming Newton-Raphson iterative process. Each Newton-Raphson iteration in turn requires evaluations of integrals to obtain state densities $N_s(V_{SC})$ and $N_d(V_{SC})$. Below we show how these calculations can be vastly simplified without a significant loss of accuracy. The typical dependence of non-equilibrium mobile charge density at the source, calculated from equations(3) and (10) , is illustrated in figure 2. Corresponding graphs for the drain charge density have similar shapes. Figure 2 also shows sample piece-wise linear approximations of the charge density curves. As explained below, this numerical linearization, where piece-wise linear regions are expressed by equations (15) and (16), leads to vast CPU time savings as it completely eliminates the need for Newton-Raphson iterations and numerical evaluation of state density integrals.

Unlike what has been proposed in a recent publication [8], that a three-piece linear approximation of the state densities should rely on symbolic calculations of slopes and intersection points from CNT parameters, the approach we suggest here is to not to link the slopes and intersection points to CNT parameters directly but rather to use an arbitrary number of them and adjust their slopes and intersection points to maximize the overall drain current characteristic accuracy. In the next section we show test results with this approach applied to a 3-range and 5-range piecewise linear approximation of the charge densities. This, purely numerical rather than symbolic, approach not only gives the model developer more control over the accuracy but also leads to a dramatic saving in the processing time.

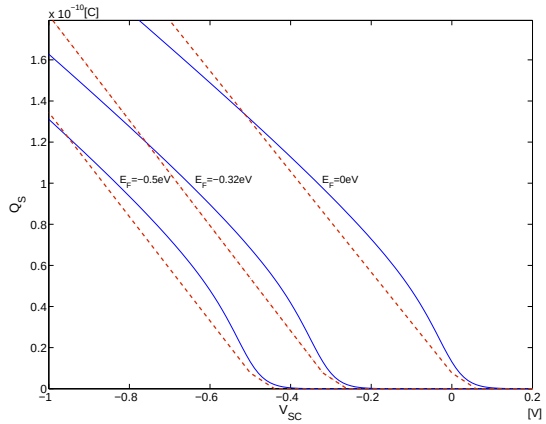

Figure 2. Charge density dependence on self-consistent voltage for Ef=0, -0.32 and -0.5 eV. Dashed lines represent a sample linearized approximation.

The CPU time is reduced by up to almost four orders of magnitude compared with the theoretical model [1] implemented in FETToy [9], as demonstrated in section 3.

The drain current can be approximated from the ballistic CNT transport theory [1, 9] as follows

$$I_{DS} = I_0 \left[\mathcal{F}_0(\frac{U_{SF}}{kT}) - \mathcal{F}_0(\frac{U_{DF}}{kT}) \right] \tag{12}$$

where $\mathcal{F}_0$ represents the Fermi-Dirac integral of order 0 and the current I_0 is expressed as

$$I_0 = \frac{2qkT}{\pi\hbar} \tag{13}$$

where k is Boltzmann's constant, T is the temperature and $\hbar$ is reduced Planck's constant.

A closed-form approximation of the Fermi-Dirac integral can be used to avoid numerical integration, e.g. [12]

$$\mathcal{F}_0(\eta) = log\,(1 + e^{\eta}) \tag{14}$$

The proposed model relies on a linear approximation of the mobile charge dependence on the self-consistent voltage V_{SC} (figure 2) where each linear range in the charge density curve can be expressed as

$$Q_s(V_{SC}) \approx -A_s(qV_{SC} - E_F) + Q_{scs0} \tag{15}$$

and

$$Q_d(V_{SC}) \approx -A_d(qV_{SC} - E_F) + Q_{scd0} \tag{16}$$

for the source and drain mobile charges correspondingly. A_s, A_d, Q_{scs0} and Q_{scd0} represent constant model parameters which may be optimally adjusted for each linear range such that the I_{DS} is predicted as accurately as possible.

The self-consistent voltage V_{SC} can now be approximated explicitly from the following closed-form linear formula

$$V_{SC} \approx \frac{Q_t + Q_{scs0} + Q_{scd0}}{C_T} \tag{17}$$

where $C_T = C_\Sigma + q(A_s + A_d)$.

3. Model performance

The model was evaluated by comparing its I_{DS} prediction accuracy and execution speed with those exhibited by FETToy [9]. As the FETToy MATLAB script is freely available on line, we have used it and replaced FETToy's I_{DS} code with our own algorithm for the fast model as outlined above. In this way we maintained equal conditions for the purpose of the performance evaluation in both models, including the same CNT parameter values as in the original FETToy script [9], as well as identical set up and output code. Comparative results showing families of drain current characteristics calculated for three and five piece-wise regions for the mobile charge density approximation assuming a 1nm CN diameter. Comparative results at $Ef = -0.32eV$ and $T = 300K$ are shown in figures 3 and (4 correspondingly. Figures 5 and 6 illustrate comparative I_{DS} characteristics for a 5-range linear approximation and different Fermi levels $Ef = 0eV$ and $Ef = -0.5eV$ at $T = 300K$ correspondingly.

CPU times were measured by running the FETToy script in two versions, the original one, which implements an accurate theoretical model [1] and the modified version where I_{DS} was calculated from the equations derived in the previous section. Results indicate an almost four-order of magnitude speed-up as shown in table 1. For accurate measurement, an extra outermost loop was added to run both algorithms 100 times. The code to generate output plots was switched off for the purpose of the CPU comparison. It has not been possible to compare our CPU times with the symbolic piece-wise linear approach mentioned above [8] as the authors have not reported how much CPU time their model uses apart from indicating that their execution time is fast.

Table 2 illustrates the relative difference in I_{DS} values in terms of the average root-mean square (RMS) error between the FETToy results and those calculated for the proposed fast model. RMS errors were measured for 3 and 5 linear range approximations of the charge densities for $Ef = 0, -0.32, -0.5$ eV and $T = 300$K. Similarly, table 3 shows average RMS errors for I_{DS} characteristics calculated at $Ef = -0.32eV$ and two different temperatures

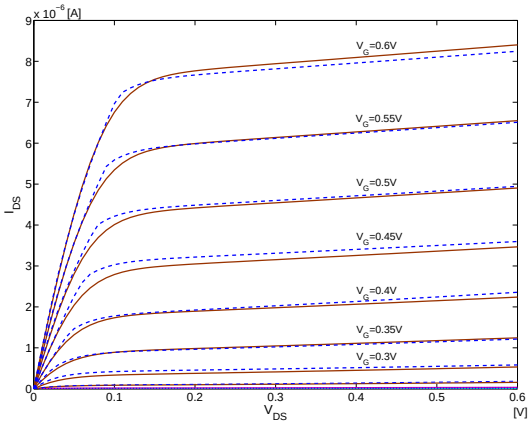

Figure 3. Drain current characteristics for Ef=-0.32eV at T=300K. Solid lines - FETToy, dashed lines - proposed model using 5 linear ranges of the charge densities.

Table 1. Average CPU times per 100 CNT characteristic families.

FETToy	Proposed CNT model	
	3 linear ranges	5 linear ranges
1287.45 sec	0.16 sec	0.71 sec

$T = 150K$ and $T = 450K$. The tests confirm that the linear approximation in the fast model causes a slight loss of accuracy, normally within a few percent but exceeding 10% in extreme cases. Results in table 2 show that the 5-range approximation is for some V_G and V_{DS} values about twice as accurate as the 3-range one, at some CPU time expense as shown in table 1.

4. SPICE-compatible companion model of $I_{DS}(V_G, V_D, V_S)$

The model presented in the previous section has a form suitable for a direct implementation in a SPICE-like simulator. SPICE and most other analog and mixed-signal circuit simulators formulate their analog system equation set from companion models which contain derivatives of model equations with regards to the unknown variables. Partial derivatives of I_{DS} with regard to the terminal voltages V_G, V_S and V_D can be obtained in analytical form as follows

$$\frac{\partial I_{DS}}{\partial V_G} = \frac{\partial I_{DS}}{\partial U_{SF}} \frac{\partial U_{SF}}{\partial V_G} + \frac{\partial I_{DS}}{\partial U_{DF}} \frac{\partial U_{DF}}{\partial V_G} \qquad (18)$$

Table 2. Average RMS errors in I_{DS} characteristic comparisons for 3 and 5 linear ranges in charge density approximation for T=300K and Ef=0,-0.32,-0.5eV.

$V_G[V]$	Ef = 0eV		Ef = -0.32eV		Ef = -0.5ev	
	Linear ranges					
	3	5	3	5	3	5
0	4.4%	4.4%	0.0%	0.0%	0.0%	0.0%
0.05	3.6%	3.6%	0.0%	0.0%	0.0%	0.0%
0.1	2.7%	2.7%	0.0%	0.0%	0.1%	0.1%
0.15	2.9%	2.9%	0.0%	0.0%	0.1%	0.1%
0.2	2.2%	2.2%	0.3%	0.3%	0.1%	0.1%
0.25	2.0%	2.0%	1.7%	1.7%	0.1%	0.1%
0.3	1.9%	1.0%	5.0%	2.6%	0.1%	0.1%
0.35	1.4%	0.5%	0.9%	0.5%	0.1%	0.1%
0.4	0.9%	0.2%	1.4%	0.5%	0.2%	0.2%
0.45	0.5%	0.3%	1.2%	0.8%	1.5%	1.4%
0.5	1.2%	1.6%	0.6%	0.3%	5.1%	3.1%
0.55	1.9%	1.8%	0.3%	0.2%	0.9%	0.6%
0.6	2.6%	2.0%	0.6%	0.2%	1.4%	0.4%

Table 3. Average RMS errors in I_{DS} characteristic comparisons for 3 and 5 linear ranges in charge density approximation for Ef=-0.32eV and T=150,450K.

V_G [V]	T = 150K		T = 450K	
	Linear ranges			
	3	5	3	5
0.0	10.0%	10.0%	12.5%	12.5%
0.05	9.4%	9.4%	12.4%	12.4%
0.1	8.0%	8.0%	12.2%	12.2%
0.15	6.2%	6.2%	11.8%	11.8%
0.2	4.5%	4.5%	10.9%	10.9%
0.25	4.0%	4.0%	8.9%	8.9%
0.3	3.4%	3.5%	4.8%	5.9%
0.35	3.1%	2.2%	4.9%	4.8%
0.4	2.6%	2.3%	4.3%	3.0%
0.45	2.4%	1.0%	3.4%	2.0%
0.5	2.2%	0.8%	2.3%	1.8%
0.55	2.0%	1.9%	1.4%	1.6%
0.6	1.8%	2.2%	0.9%	1.4%

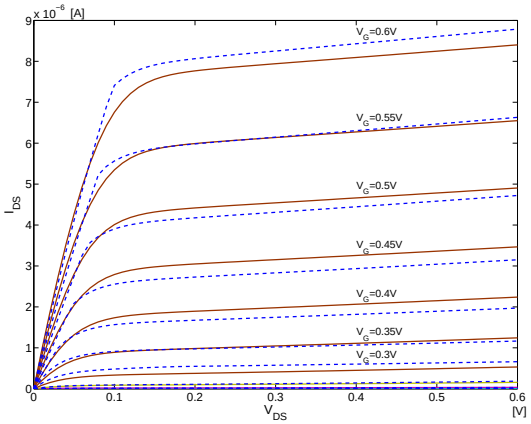

Figure 4. Drain current characteristics for Ef=-0.32eV at T=300K. Solid lines - FETToy, dashed lines - proposed model using 3 linear ranges of the charge densities.

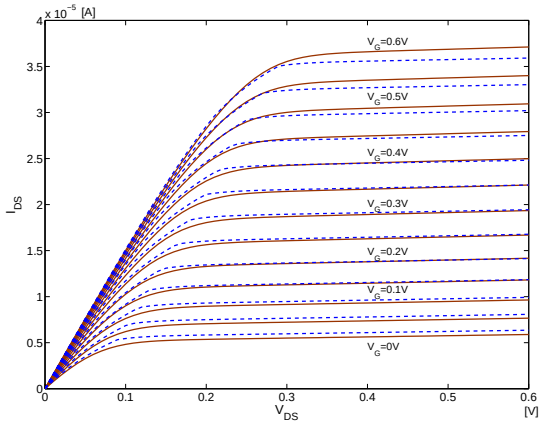

Figure 5. Drain current characteristics for Ef= 0 eV at T=300K. Solid lines - FETToy, dashed lines - proposed model using 5 linear ranges of the charge densities.

$$\frac{\partial I_{DS}}{\partial V_S} = \frac{\partial I_{DS}}{\partial U_{SF}}\frac{\partial U_{SF}}{\partial V_S} + \frac{\partial I_{DS}}{\partial U_{DF}}\frac{\partial U_{DF}}{\partial V_S} \tag{19}$$

$$\frac{\partial I_{DS}}{\partial V_D} = \frac{\partial I_{DS}}{\partial U_{SF}}\frac{\partial U_{SF}}{\partial V_D} + \frac{\partial I_{DS}}{\partial U_{DF}}\frac{\partial U_{DF}}{\partial V_D} \tag{20}$$

Equations (5) and (6) yield

$$\frac{\partial U_{SF}}{\partial V_G} = \frac{\partial U_{DF}}{\partial V_G} = -q\frac{\partial V_{SC}}{\partial V_G} \tag{21}$$

$$\frac{\partial U_{SF}}{\partial V_S} = -q\frac{\partial V_{SC}}{\partial V_S} \tag{22}$$

$$\frac{\partial U_{SF}}{\partial V_S} = -q\frac{\partial V_{SC}}{\partial V_S} \tag{23}$$

$$\frac{\partial U_{DF}}{\partial V_S} = -q\left(1 + q\frac{\partial V_{SC}}{\partial V_S}\right) \tag{24}$$

$$\frac{\partial U_{DF}}{\partial V_D} = -q\left(1 + q\frac{\partial V_{SC}}{\partial V_D}\right) \tag{25}$$

From equation (7) and the linearised approximation defined by equations (15) and (16), V_{SC} derivatives are constant in each piece-wise region and can be estimated as:

$$\frac{\partial V_{SC}}{\partial V_G} = \frac{C_G}{C_\Sigma + q(A_s + A_d)} \tag{26}$$

$$\frac{\partial V_{SC}}{\partial V_S} = \frac{C_S}{C_\Sigma + q(A_s + A_d)} \tag{27}$$

$$\frac{\partial V_{SC}}{\partial V_D} = \frac{C_S}{C_\Sigma + q(A_s + A_d)} \tag{28}$$

Hence, from the above equations, equation (12) and equation (14), the drain current derivatives required to create a companion model for an analog circuit solver can be estimated as

$$\frac{\partial I_{DS}}{\partial V_G} = \frac{qI_0}{kT}\frac{C_G}{C_T}\left(\frac{1}{1+e^{\frac{U_{DF}}{kT}}} - \frac{1}{1+e^{\frac{U_{DF}}{kT}}}\right) \tag{29}$$

$$\frac{\partial I_{DS}}{\partial V_S} = \frac{qI_0}{kT}\frac{C_S}{C_T}\left(\frac{1}{1+e^{\frac{U_{DF}}{kT}}} - \frac{1}{1+e^{\frac{U_{DF}}{kT}}}\right) \tag{30}$$

$$+\frac{qI_0}{kT}\frac{1}{1+e^{\frac{U_{DF}}{kT}}} \tag{31}$$

and

$$\frac{\partial I_{DS}}{\partial V_D} = \frac{qI_0}{kT}\frac{C_D}{C_T}\left(\frac{1}{1+e^{\frac{U_{DF}}{kT}}} - \frac{1}{1+e^{\frac{U_{DF}}{kT}}}\right) \tag{32}$$

$$+\frac{qI_0}{kT}\frac{1}{1+e^{\frac{U_{DF}}{kT}}} \tag{33}$$

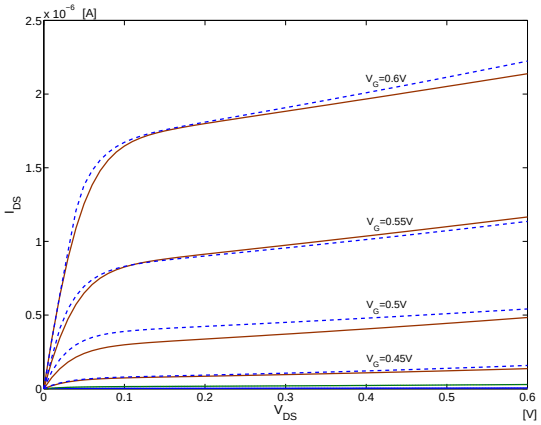

Figure 6. Drain current characteristics for Ef= -0.5 eV at T=300K. Solid lines - FETToy, dashed lines - proposed model using 5 linear ranges of the charge densities.

5. Conclusion

We have proposed a new, fast numerical CNT model suitable for a direct implementation in SPICE-like simulators. Results provide further evidence to support the recent suggestion [8] to avoid the use of numerical integration when calculating charge densities in the CNT model, leading to significant speed up in the model simulation. We have proposed to apply an arbitrary number of linear approximation regions to the non-equilibrium mobile charge densities rather than the symbolic three-piece form [8]. The mobile charge densities are represented in a form suitable for a direct implementation in a circuit model. When compared with FETToy [9], a reference theoretical CNT model, we have demonstrated that the proposed approximation approach leads to a dramatic computational cost saving without sacrificing the modeling accuracy. Findings of this research contribute towards the current efforts in nanoelectronic circuit design that include development of fast and accurate CN FET models with the aim to enable circuits with large numbers of such devices to be simulated efficiently and accurately. Future work will involve development of automated optimization techniques for the mobile charge density piece-wise linear approximations such that the I_{DS} prediction accuracy can be further increased while maintaining the fast execution speed.

References

[1] A. Rahman, Jing Guo, S. Datta, and M.S. Lundstrom. Theory of ballistic nanotransistors. *Electron Devices, IEEE*, 50(9):1853–1864, September 2003.

[2] P. Avouris, J. Appenzeller, R. Martel, and S.J. Wind. Carbon nanotube electronics. *Proceedings of the IEEE*, 91(11):1772–84, November 2003.

[3] Arash Hazeghi, Tejas Krishnamohan, and H.-S. Philip Wong. Schottky-Barrier Carbon Nanotube Field-Effect Transistor Modeling. In *Sixth IEEE Conference on Electron Devices*, volume 54, Lausanne, Switzerland, March 2007.

[4] T. Dang, L. Anghel, and R. Leveugle. Cntfet basics and simulation. In *IEEE Int. conf. on Design and Test of Integrated Systems in Nanoscale Technology (DTIS)*, Tunis, Tunisia, 5-7 September 2006.

[5] C. Dwyer, M. Cheung, and D.J. Sorin. Semi-empirical SPICE models for carbon nanotube FET logic. In *4th IEEE Conference on Nanotechnology*, Munich, Germany, 16-19 Aug. 2004.

[6] A. Raychowdhury, S. Mukhopadhyay, and K. Roy. A circuit-compatible model of ballistic carbon nanotube field-effect transistors. *Applied Physics Letters*, 23(10):1411–20, October 2004.

[7] B.C. Paul, S. Fujita, M. Okajima, and T. Lee. Modeling and analysis of circuit performance of ballistic CNFET. In *2006 Design Automation Conference*, San Francisco, CA, USA, 24-28 July 2006.

[8] H. Hashempour and F. Lombardi. An efficient and symbolic model for charge densities in ballistic carbon nanotube fets. *IEEE-NANO*, 1:17–20, 2006.

[9] Anisur Rahman, Jing Wang, Jing Guo, Sayed Hasan, Yang Liu, Akira Matsudaira, Shaikh S. Ahmed, Supriyo Datta, and Mark Lundstrom. Fettoy 2.0 - on line tool, 14 February 2006. `https://www.nanohub.org/resources/220/`.

[10] M.H. Yang, K.B.K. Teo, L. Gangloff, W.I. Milne, D.G. Hasko, Y. Robert, and P. Legagneux. Advantages of top-gate, high-k dielectric carbon nanotube field-effect transistors. *Applied Physics Letters*, 88(11):113507–1–3, March 2006.

[11] P.L. McEuen, M.S. Fuhrer, and Hongkun Park. Single-walled carbon nanotube electronics. *Nanotechnology, IEEE Transactions*, 1(1):78–845, March 2002.

[12] M. Galassi, J. Davies, J. Theiler, B. Gough, G. Jungman, Booth M., and F. Rossi. *GNU Scientific Library Reference Manual - Revised Second Edition (v1.8)*. Network Theory Ltd, August 2006.